CrossMark

Amblyomin-X induces ER stress, mitochondrial dysfunction, and caspase activation in human melanoma and pancreatic tumor cell

Katia L. P. Morais[1,2] · Mario Thiego Fernandes Pacheco[1] · Carolina Maria Berra[3] ·
Rosemary V. Bosch[1] · Juliana Mozer Sciani[1] · Roger Chammas[4] ·
Renata de Freitas Saito[4] · Asif Iqbal[1] · Ana Marisa Chudzinski-Tavassi[1,2]

Abstract During the last two decades, new insights into proteasome function and its role in several human diseases made it a potential therapeutic target. In this context, Amblyomin-X is a Kunitz-type FXa inhibitor similar to endogenous tissue factor pathway inhibitor (TFPI) and is a novel proteasome inhibitor. Herein, we have demonstrated Amblyomin-X cytotoxicity to different tumor cells lines such as pancreatic (Panc1, AsPC1BxPC3) and melanoma (SK-MEL-5 and SK-MEL-28). Of note, Amblyomin-X was not cytotoxic to normal human fibroblast cells. In addition, Amblyomin-X promoted accumulation of ER stress markers (GRP78 and GADD153) in sensitive (SK-MEL-28) and bortezomib-resistant (Mia-PaCa-2) tumor cells. The intracellular calcium concentration $[Ca^{2+}]_i$ was slightly modulated in human tumor cells (SK-MEL-28 and Mia-PaCa-2) after 24 h of Amblyomin-X treatment. Furthermore, Amblyomin-X induced mitochondrial dysfunction, cytochrome-c release, PARP cleavage, and activation of caspase cascade in both human tumor (SK-MEL-28 and Mia-PaCa-2) cells. These investigations might help in further understanding of the antitumor properties of Amblyomin-X.

✉ Ana Marisa Chudzinski-Tavassi
ana.chudzinski@butantan.gov.br

[1] Biochemistry and Biophysics Laboratory, Butantan Institute, Av. Vital Brazil, 1500, São Paulo, SP 05503-900, Brazil

[2] Department of Biochemistry, Federal University of São Paulo, São Paulo, SP, Brazil

[3] Biochemistry Department, Institute of Chemistry, University of São Paulo, São Paulo, Brazil

[4] Experimental Oncology Medical Investigation Laboratory – LIM/24, University of São Paulo School of Medicine, São Paulo, SP, Brazil

Abbreviations

ER	Endoplasmic reticulum
$[Ca^{2+}]_i$	Intracellular calcium concentration
ERAD	ER-associated degradation
UPR	Unfolded protein response
GRP78	78 kDa glucose-regulated protein; kinase-like ER kinase (PERK), the inositol requiring kinase 1 alpha (IRE1α), and the transcription factor-activating transcription factor 6 (ATF6)
eIF2α	Alpha subunit of translation initiation factor
GADD153	Nuclear transcription factors of growth arrest and DNA damage
TRAF2	Tumor necrosis factor TNF receptor-associated factor (TRAF) 2
JNK	c-Jun-N-terminal kinase
^{123}Rh	Rhodamine 123
TAPS	Thapsigargin
PARP	A 116 kDa nuclear poly (ADP-ribose) polymerase
TFPI	Tissue factor pathway inhibitor
TF	Tissue factor
KRAS	v-Ki-ras2 Kirsten rat sarcoma viral oncogene homolog
PERK	Protein kinase-like ER kinase
IRE1α	Inositol requiring kinase 1 alpha
ATF6	Transcription factor-activating transcription factor 6
ATF4	Actor-activating transcription factor 4

✿ Springer

Introduction

The proteasome is a large protein complex responsible for regulation of intracellular proteolysis in all eukaryotic cells. Thereby, it plays an essential role in the regulation of the cellular processes, including protein quality control, cell cycle progression, differentiation, signal transduction, apoptosis, gene expression, and antigen processing [1–3]. Thus, a dysfunction of proteasome activity has detrimental effect on cell homeostasis. In humans, proteasome deregulation has numerous implications in pathologies such as cancer, autoimmune diseases, neurodegenerative diseases, and viral infections [1–3], rendering it as a potential therapeutic target [2]. A proteasome inhibitor bortezomib is approved by FDA for the treatment of multiple myeloma, and several others are in clinical trials [3].

Cell death induced by proteasome inhibitors could involve endoplasmic reticulum (ER) stress [4–7]. Important steps in the synthesis of the proteins directed to the secretory pathway or to plasma membrane are processed in the ER-lumen, such as folding and post-translational modifications [8, 9]. However, if correct folding is not reached, the first quality control system (calnexin/calreticulin) works to bring proteins in the correct folding [8]. Many misfolded proteins undergo this quality control system and can be eliminated via the proteasome, by a mechanism known as endoplasmic reticulum-associated protein degradation (ERAD) [10, 11]. The inhibition of this process ultimately leads to the accumulation and aggregation of proteins in the ER and the induction of ER stress [8, 11]. Thus, ERAD fine-tuning is essential for proteostasis [10]. Despite no direct association, ERAD could share common pathways with unfolded protein response (UPR), for instance, IRE1-dependent transcription factor XBP1 codes for several ERAD-related genes [10, 12]. Overall, those pathways underline key ubiquitin–proteasome system functions related to un/misfolded protein disposal and cell stress response.

During UPR activation, the chaperone 78 kDa glucose-regulated protein (GRP78) is released from three ER transmembrane proteins: protein kinase-like ER kinase (PERK); the inositol requiring kinase 1 alpha (IRE1α); and the transcription factor-activating transcription factor 6 (ATF6) [13, 14]. The ER transmembrane proteins IRE1α and PERK undergo dimerization and auto-phosphorylation and are consequently activated that redirect alternative transcription of chaperones and transcription factors, such GRP78 and factor-activating transcription factor 4 (ATF4) [15]. PERK phosphorylates the eukaryotic translation initiation factor (eIF)2α and results in a global attenuation of protein translation. These events help the cell to cope with accumulated unfolded proteins and restore ER homeostasis. In parallel, ATF6 is transported to the Golgi, where it is sequentially cleaved by Golgi resident proteases, resulting in the release of cytosolic domain of ATF6, which goes to the nucleus to activate the transcription of target genes (GRP78, GADD153, calreticulin) [16]. However, failure to relieve prolonged or severe ER stress, triggers apoptosis [8].

If ER stress is persistent or severe and ER homeostasis is not restored, UPR activates cell death pathways. One of ER stress-induced cell death pathways is mediated by IRE1 that can interact with the adaptor protein of TNF receptor-associated factor 2 (TRAF2), leading to the activation of apoptosis signal-regulating kinase 1 [17]. This might mediate apoptosis in response to ER stress by activation of c-Jun-N-terminal kinase (JNK). The complex IRE1α/TRAF2 also activates ER-resident caspase-4 [17]. Furthermore, ATF4 can lead to the upregulation of nuclear transcription factors of growth arrest and DNA damage (GADD153). This able cells to (i) transcriptionally down-regulate the levels of Bcl-2 and upregulate DR5; (ii) cause cell cycle arrest; (iii) sensitize the mitochondria to pro-apoptotic Bcl-2 family proteins; (iv) lead to a depletion of the cellular glutathione levels and increase levels of reactive oxygen species [18–20]. In addition, calcium released from the ER is rapidly taken up by the mitochondria, where it leads to collapse of inner membrane potential, cytochrome-c release, caspase cascade activation, and subsequent initiation of apoptosis [21–23].

In this context, Amblyomin-X is a homolog of Kunitz-type protein identified in the transcriptome of the salivary glands from the adult *Amblyomma cajennense* tick [24, 25]. The recombinant protein form of Amblyomin-X has presented antitumor activity via induction of apoptosis and inhibition of proteasome [26, 27]. The human melanoma (SK-MEL-28) and human pancreas adenocarcinoma (Mia-PaCa-2) tumor cells were a good choice to investigate the mechanism of action of Amblyomin-X, because both of them are sensitive to pro-apoptotic effects of Amblyomin-X [24]. In addition, Mia-PaCa-2 cells are resistant to bortezomib-induced apoptosis [28]. In this study, we reported pro-apoptotic effect of Amblyomin-X in these human tumor cells associated to inhibition of proteasome function, ER stress (UPR markers upregulation), mobilization of $[Ca^{2+}]_i$, mitochondrial dysfunction, PARP cleavage, and caspase-3 activation. Interestingly, none of these changes were observed in normal human fibroblast cells.

Results

Amblyomin-X induces cytotoxicity in human tumor cells

The effect of Amblyomin-X (1 μM) on cell viability of human melanoma (SK-MEL-28 and SK-MEL-5) and pancreatic (Mia-PaCa-2, Panc1, AsPC1, and BxPC3) tumor cells was investigated. After 48 h, cells treated with Amblyomin-X decreased the viability considerably as shown in Table 1. The amount of viable cells was different for both tumors cells; for example, ∼67 % of Mia-PaCa-2 and ∼29 % of metastatic-derived AsPC1 were viable after 48 h of Amblyomin-X treatment (Table 1). However, no changes in cell viability of human fibroblast were observed after 48 h of Amblyomin-X treatment (Table 1).

Amblyomin-X triggers ER stress in tumor cells

It has been reported that Amblyomin-X inhibits proteasome system [26, 27]. The inhibition of proteasome can cause ER stress, thus, we decided to assess whether Amblyomin-X could induce ER stress. A representative of human melanoma and pancreatic tumor cells lines i.e., Mia-PaCa-2 and SK-MEL-28 were selected for this study, since the effect of Amblyomin-X on the protein clearance in those tumor cells has been investigated [29]. Human fibroblast were used as non-tumor cell model.

The mRNA levels of the proteins related to the ER stress were estimated using real-time PCR. When SK-MEL-28 cells are treated with 0.5 μM of Amblyomin-X, the mRNA levels of IRE1α, ATF4, and GRP78 genes increased after 2 h and only GADD153 gene expression augmented in a time-dependent manner but was significant only after 4 h (Fig. 1a). The expression of the caspase-4 gene increased after 24 h of treatment with Amblyomin-X. On the other hand, the expression of the eIF2α gene did not increase in the SK-MEL-28 cells treated with 0.5 μM Amblyomin-X

(Fig. 1a). In Mia-PaCa-2 cells treated with 0.5 μM of Amblyomin, the expression of IRE1α and GADD153 genes increased after 24 h (Fig. 1a). The GRP78, ATF4, eIF2α, and caspase-4 genes showed no significant changes in expression when compared to their corresponding controls. Moreover, we verified the protein levels of GRP78 and GADD153 in tumor cells after Amblyomin-X treatment. The GRP78 protein levels increased in SK-MEL-28 after 4 h and in Mia-PaCa-2 after 24 h (Fig. 1b). The GADD153 protein levels increased after 24 h in both cells lines (Fig. 1b). Human fibroblast cells showed some alterations in IRE1α and eIF2α gene after 24 h of Amblyomin-X treatment (Fig. 1b). In contrast, no alterations were found in GRP78 and GADD153 protein levels in human fibroblast after Amblyomin-X treatment.

It is well established that ATF-6α and cargo proteins are transported from the ER to the Golgi apparatus through the ER-Golgi intermediate compartment (ERGIC) [30, 31] and ERGIC-53 is a specific marker for ERGIC [31]. As shown in Fig. 1c, anti-ATF-6α antibody stained cytoplasmic in "Ctrl" tumor cells. In contrast, ATF-6α moved toward and reached the nucleus of tumor cells treated with Amblyomin-X. Importantly, ATF6 staining overlapped with ERGIC-53, and the images suggest close proximity to nucleus.

Amblyomin-X modulates mobilization of $[Ca^{2+}]_i$ in tumor cells

We further investigated whether treatment with Amblyomin-X would cause the mobilization of $[Ca^{2+}]_i$ in SK-MEL-28 cells using microfluorimetry. We observed a sustained but not a statistical increase in the $[Ca^{2+}]_i$, after the application of 0.5 μM of Amblyomin-X (Fig. 2a, b). In human fibroblast, no alterations were observed (Fig. 2a, b). In the positive control cells treated with TAPS (1 μM) a change in fluorescence signal was observed in both cell types. In Ctrl, cells were treated with PBS which showed no fluorescence alteration (Fig. 2a, b).

Table 1 Effect of Amblyomin-X in cell viability of different tumor cell lines

Tumor cell line	Origin	Viability
Mia-PaCa-2	Human pancreatic adenocarcinoma	67.02 ± 5.9***
Panc1	Human pancreatic epithelioid carcinoma	35.81 ± 1.2**
AsPC1	Human pancreatic adenocarcinoma	29.56 ± 1.03**
BxPC3	Human pancreatic adenocarcinoma	13.89 ± 0.50**
SK-MEL-28	Human melanoma	43.91 ± 10.5**
SK-MEL-5	Human melanoma	42.34 ± 13.75**
Human Fibroblast	Non-tumor cell	106.76 ± 10.01

Tumor cells lines were incubated with 1 μM of Amblyomin-X for 48 h, and cell viability was assessed as described in Materials and Methods. The data presented as the mean ± SD of three independent experiments

**$p \leq 0.005$, ***$p \leq 0.001$ compared with the control group (corresponding untreated cells), as determined by one-way ANOVA
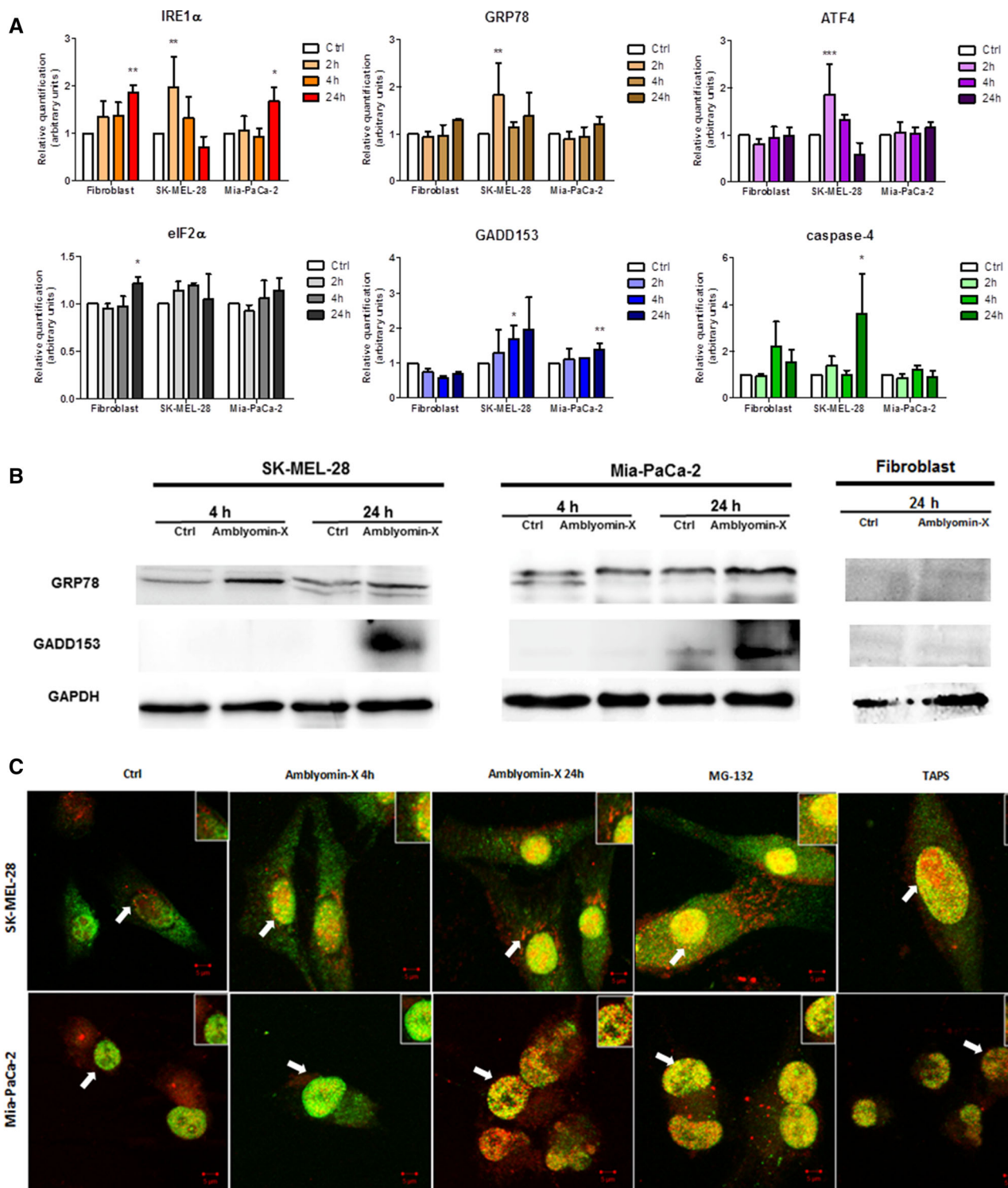
Fig. 1 Amblyomin-X induces ER stress in tumor cells. **a** Cells were treated with Amblyomin-X (0.5 μM) at the indicated times and levels of gene expression of targets related to ER stress were evaluated by real-time PCR. **b** After the indicated period of treatment, cells were lysed with RIPA buffer and 30 μg of total protein was used for the tests. Western blot analysis was performed by checking anti-GRP78, anti-GADD153, and anti-GAPDH (endogenous controls). **c** Confocal microscopy analysis of indirect immunofluorescence of ATF-6α and ERGIC53. Cells treated with vehicle (PBS), or with 0.5 μM of Amblyomin-X for 4 or 24 h, or with MG-132 (2.5 μM) and TAPS (1 μM) for 24 h each. The final overlay image is a representative of three independent experiments in which *red fluorescence* represents ATF-6α, while *green fluorescence* represents ERGIC53, and *yellow* corresponds to merging of both *red and green*. Values are mean ± SD of three independent experiments. *$p \leq 0.05$; **$p \leq 0.01$, and ***$p \leq 0001$. (Color figure online)
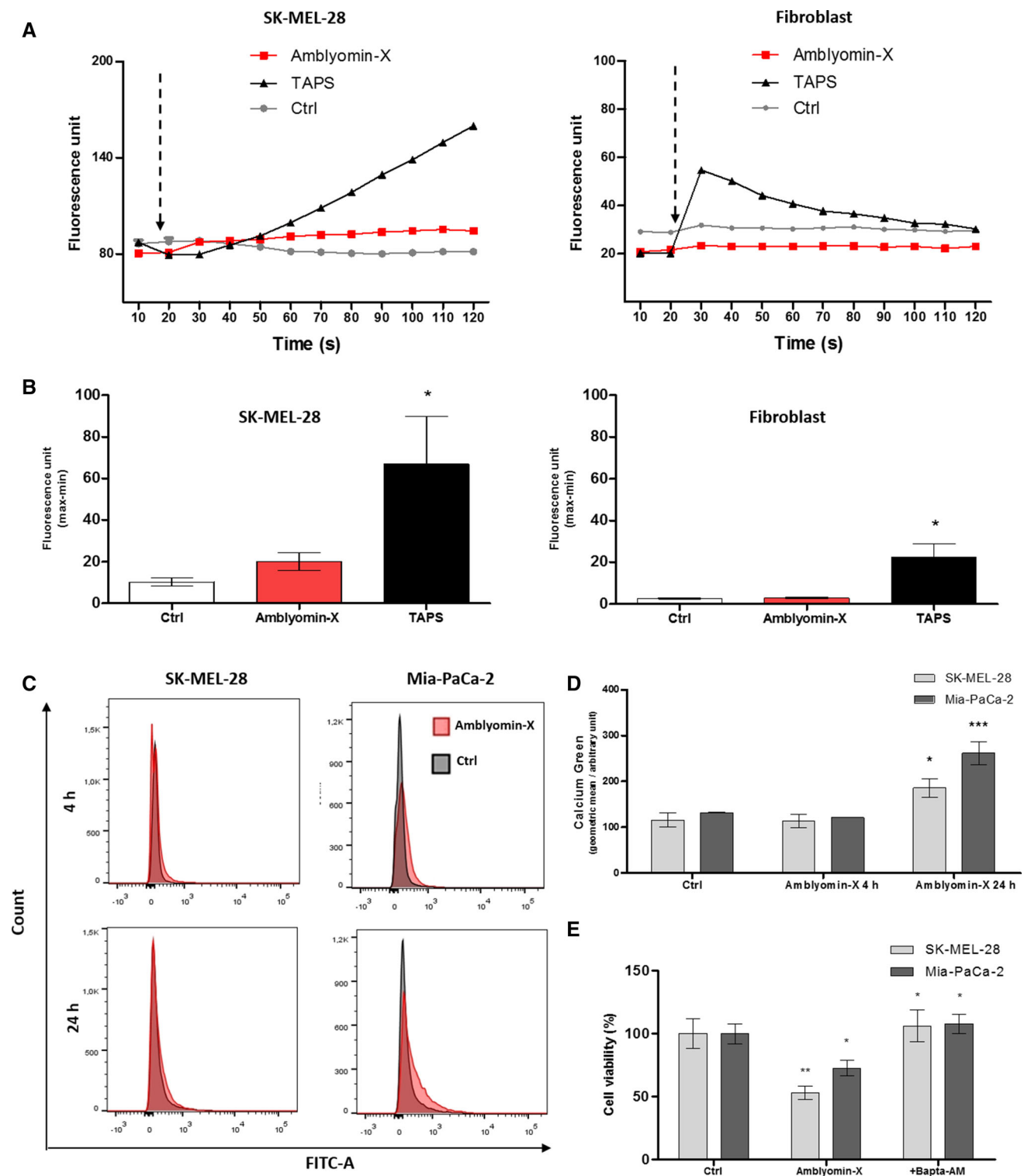
Fig. 2 Amblyomin-X increases intracellular calcium levels in SK-MEL-28 cells. **a** $[Ca^{2+}]_i$ levels of unstimulated SK-MEL-28 and human fibroblast cells were measured for 20 s, followed by addition (marked by *arrows*) of Amblyomin-X (1 μM), TAPS (1 uM), or 50 uL of PBS 1X (Ctrl), and monitored for more than 100 s by microfluorimetry. **b** Graphic representation of quantitative measurements of fluorescence intensity (max–min) obtained from **a**. **c** Cells were treated with Amblyomin-X, stained with calcium green-1, and analyzed by flow cytometry. Representative histograms are expressed in fluorescence intensity. **d** *Bars graph* and geometric mean (fluorescence intensity) values ± SD obtained from C (three independent experiments). **e** Cells were pre-incubated for 30 min with BAPTA-AM (10 μM), followed by incubation with Amblyomin-X (1 μM) for 48 h at 37 °C

Next, we assessed the mobilization of $[Ca^{2+}]_i$ in SK-MEL-28 and Mia-PaCa-2 cells at 4 and 24 h after treatment of Amblyomin-X using fluorescence calcium Green-1 AM indicator in flow cytometry. The mobilization of $[Ca^{2+}]_i$ increased in both tumor cells after 24 h of Amblyomin-X treatment compared to control (Fig. 2c, d). The pre-treatment with BAPTA-AM protected the tumor cells from Amblyomin-X cytotoxicity (Fig. 2e).

Amblyomin-X affect the mitochondria integrity

We investigated whether the Amblyomin-X causes mitochondrial dysfunction. In SK-MEL-28 and Mia-PaCa-2 cells treated with 0.5 μM of Amblyomin-X, the mitochondrial membrane changed slightly after 4 h. The mitochondrial membrane potential changed significantly in both cell lines after 24 h of its treatment with Amblyomin-X, but was more pronounced in SK-MEL-28 (Fig. 3a, b). Considering mitochondrial dysfunction induced by Amblyomin-X could result in the release of pro-apoptotic factors (such as cytochrome-c) into the cytoplasm, the cytoplasmic levels of the cytochrome-c were determined by Western blotting, which was increased after 48 h in the cell lines treated with 0.5 μM of Amblyomin-X (Fig. 3c).

Caspase cascade activation in tumor cells by Amblyomin-X

The release of cytochrome-c from mitochondria to cytoplasm causes the activation of caspase cascades via caspase-3 leading to apoptosis [32]. Thus, we pre-incubated tumor cells for 2 h with pan caspase inhibitor ZVAD-FMK. Subsequently, Amblyomin-X was added to the tumor cells and grown for further 48 h at 37 °C as discussed in materials and methods. Tumor cells overcome cytotoxicity of Amblyomin-X, bringing the viability to ∼100 % in SK-MEL-28 and ∼92 % in Mia-PaCa-2 cells (Fig. 4a). Likewise, when tumor cells were pre-incubated with caspase-3 inhibitor DEVD-CHO, cell viability was ∼86 % in SK-MEL-28 and ∼87 % in Mia-PaCa-2 cells. When those tumor cells were not pre-treated with caspases inhibitors, cell viability was ∼45 % in SK-MEL-28 and ∼60 % in Mia-PaCa-2 cells treated with 0.5 μM Amblyomin-X (Fig. 4a).

We also quantified caspase 3/7 activity measuring the fluorogenic response resulting from DEVD peptide cleavage. As shown in Fig. 4b, c, Amblyomin-X increased caspase 3/7 activity compared to negative controls. MG-132 and TAPS were used as positive control.

Next, we determined PARP cleavage using Anti-PARP antibody as discussed in materials and methods. PARP is a 116-kDa nuclear (ADP-ribose) polymerase involved in DNA repair predominantly in response to environmental stress [33]. This protein could be cleaved by caspase-3 and 7 [34, 35] facilitating disassembling of the cellular components and this serves as a marker for cells undergoing apoptosis [33]. We evaluated PARP cleavage in tumor cells treated with Amblyomin-X. A cleaved PARP band observed in SK-MEL-28 cell after both 24 and 48 h of Amblyomin-X treatment (Fig. 4d). In Mia-PaCa-2 cells, a faint PARP cleavage band was observed after 24 h, which becomes prominent after 48 h of Amblyomin-X treatment (Fig. 4d). In human fibroblast, cleaved PARP band was not detected (Fig. 4d).

Discussion

Recently, it has been demonstrated that Amblyomin-X induces apoptosis in murine and human tumor cell lines [26, 27]. Herein, we demonstrated unprecedented results of Amblyomin-X cytotoxic effect on four tumor cells lines (Panc1, BxPC3, AsPC1, and SK-MEL-5). The amount of viable cells was different for both tumors cells treated with Amblyomin-X, which could be associated to the features of these cells. For example, Mia-PaCa-2 tumor cells derived from the pancreas adenocarcinoma of a 65-year-old man do not express measurable amounts of carcinoembryonic antigen [36, 37]. On the other hand, AsPC1 cells obtained from a 62-year-old woman produce abundant mucin as well as carcinoembryonic antigen [36, 38]. Human pancreatic cells sensitive to Amblyomin-X (Table 1) have mutation in the KRAS (v-Ki-ras2 Kirsten rat sarcoma viral oncogene homolog) and BxPC-3 is the wild-type exception [36]. Amblyomin-X sensitive human melanoma cells have mutant BRAF gene that increases kinase activity of BRAF, leading to constitutive activation of the RAS-RAF-MEK-ERK pathway and thus uncontrolled tumor proliferation [39, 40]. Obviously, the features of cells tested generate different levels of migration, invasion, tumorigenicity, and chemosensitivity. Despite that, all cells lines were sensitive to Amblyomin-X. SK-MEL-28 is sensitive to bortezomib [41], but Mia-PaCa-2, Panc1, and AsPC1 are resistant to this proteasome inhibitor [28]. In general, bortezomib-resistant cells overexpressed the β5 subunit (a target of bortezomib and have chymotrypsin-like activity) [42], which has a mutation in the binding site for bortezomib [42] or in downstream protein of the enzymatic complex [43]. In fact, Amblyomin-X inhibits the trypsin-like activity of the proteasome in tumor cells and indicates a similar interaction with β2 subunit, which is under investigation. Thereby, proteasome inhibition and/or other but yet unknown actions had made pancreatic cells sensitive to Amblyomin-X. These findings together with previous studies suggest that Amblyomin-X could function as a broad-spectrum antitumor drug. Of note, no alterations in
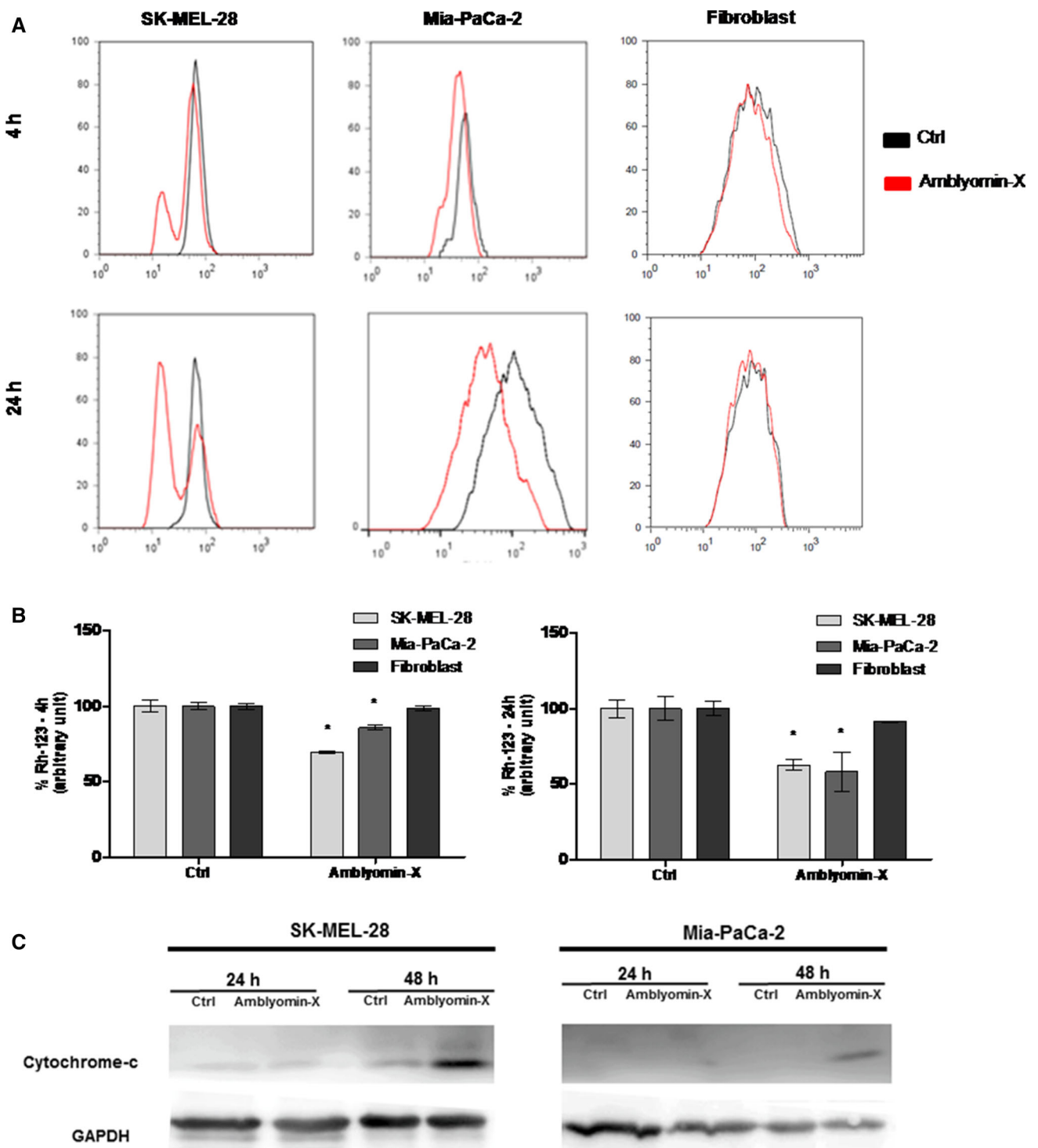
Fig. 3 Mitochondrial dysfunction induced by Amblyomin-X in tumor cells. **a** Histogram representing the mitochondrial membrane potential. Cells were treated with Amblyomin-X (0.5 μM) for 4 h and 24 h. **b** *Bars graph* (fluorescence intensity) values ± SD obtained from **a** (three independent experiments). **c** After the indicated periods of treatments, cells were lysed. The cytoplasm and membrane were separated and 30 μg of cytoplasmic protein fractions was separated on SDS-PAGE. The Western blot of the samples was performed using anti-cytochrome-c and anti-GAPDH (endogenous control)

cell viability of human fibroblast were observed, suggesting that Amblyomin-X is preferentially cytotoxic to tumor cells.

Here, we selected SK-MEL-28 and Mia-PaCa-2 in this study, since the role Amblyomin-X in protein clearance in these tumor cells have already been demonstrated [26, 29].
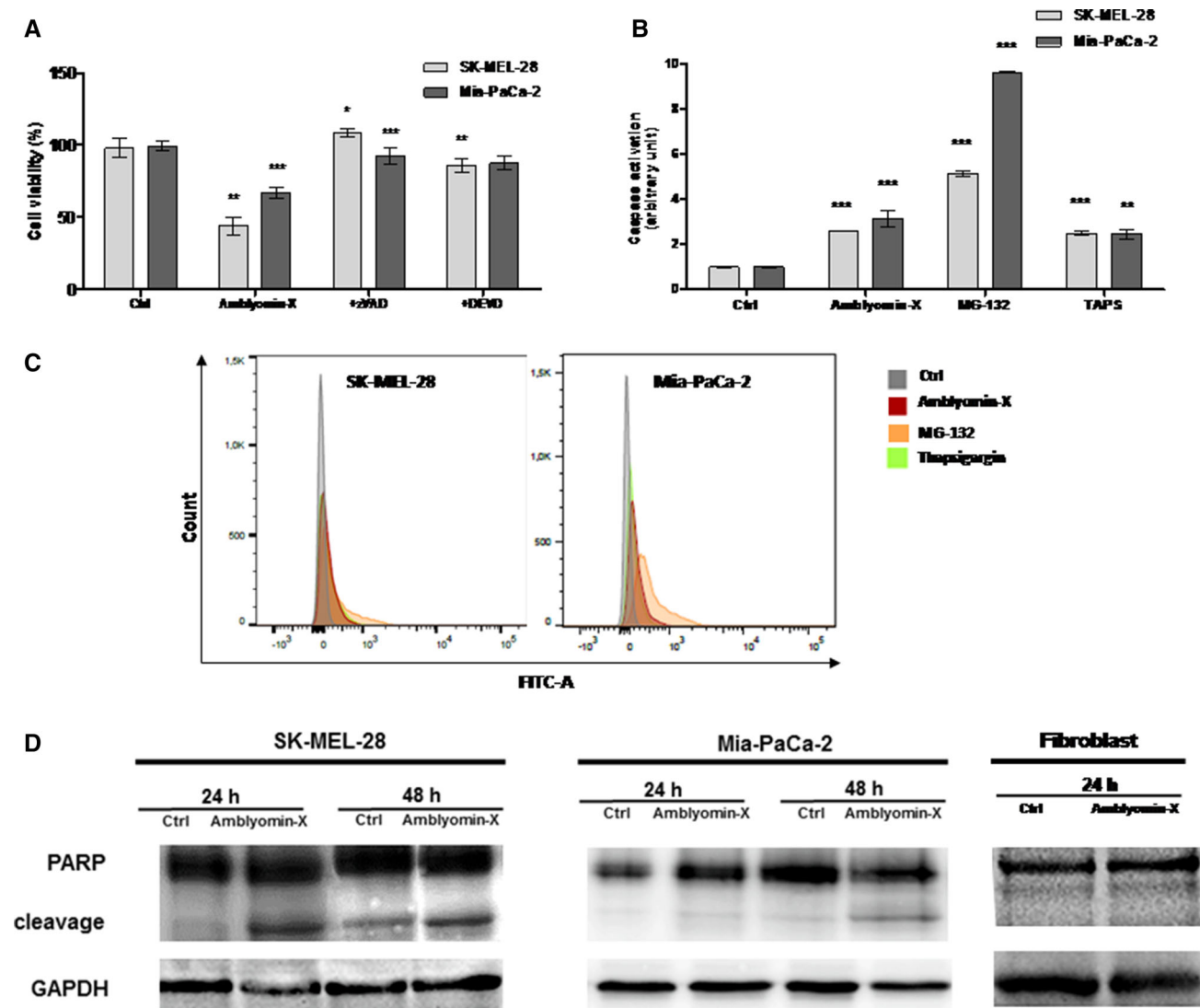
Fig. 4 Caspase cascade activation after Amblyomin-X treatment in tumor cells. **a** Cells were pre-incubated for 2 h with ZVAD-FMK (50 μM) or DEVD-CHO (10 μM) followed by incubation with Amblyomin-X (1 μM) for 48 h at 37 °C. **b** Caspase activity was measured using CellEvent™ Caspase-3/7 Green Detection Reagent (Molecular Probes), according to manufacturer's instructions. Cells treated with vehicle (PBS), or 0.5 μM of Amblyomin-X for 48 h, or with MG-132 (2.5 μM) and TAPS (1 μM) for 24 h each. Then, cells were stained with CellEvent™ Caspase-3/7 Green Detection Reagent and were analyzed by flow cytometer. **c** *Bars graph* (fluorescence intensity) values $\pm$ SD obtained from B (three independent experiments). **d** After the period of treatment, cells were lysed with RIPA buffer and 30 μg of protein extract was separated on SDS-PAGE. Western blot analysis were performed using anti-PARP and anti-GAPDH (endogenous control). $*p \leq 0.05$, $**p \leq 0.01$, and $***p \leq 0.001$ (Ctrl vs Amblyomin-X or Amblyomin-X vs inhibitors)

In fact, the data showed ER homeostasis disruption in tumor cells, since expressions of some genes of UPR and GRP78/GADD153 protein levels were elevated by Amblyomin-X treatment, as well as ATF-6α transport. An interesting point was the onset of ER stress responses (UPR gene expression at 2 h and GRP78 proteins levels at 4 h) in SK-MEL-28 cells prior to that induced via proteasome inhibition by Amblyomin-X. Thus, we cannot rule out the signaling independent proteasome inhibition. In fact, we need more investigation regarding ERAD process in tumor cells treated with Amblyomin-X. The changes in human fibroblast cells after Amblyomin-X treatment were different from those observed in tumor cells, i.e., the IRE1α and eIF2α levels increased but there was no modulation in GRP78/GADD153 levels.

In addition, perturbations of ER could compromise its function because it is one of the major intracellular Ca^{2+} storages. We observed no increase in $[Ca^{2+}]_i$ immediately after Amblyomin-X application in SK-MEL-28 cells (Fig. 2a, b), but not in human fibroblast cells. However, we noticed that the increase in $[Ca^{2+}]_i$ induced by Amblyomin-X was not transient, but proportional to the

incubation time. In SK-MEL-28 cells and Mia-PaCa-2, this phenomenon was observed after 24 h of Amblyomin-X treatment (Fig. 2c, d). The blocking of Amblyomin-X cytotoxicity by BAPTA-AM indicates that calcium released from intracellular storage (ER, mitochondria) to cytoplasm plays an important role in mode of action of Amblyomin-X.

In addition, Amblyomin-X treatment promoted mitochondrial dysfunction only in tumor cells, indicating the involvement of the intrinsic pathway of apoptosis. Several antitumor drugs have been reported to work via activation of the intrinsic pathway of apoptosis [32]. The results supported our prediction because cytochrome-c released in tumor cells were treated with Amblyomin-X, however, only after 48 h of treatment. This suggests that no adequate response was achieved to generate drastic changes in mitochondrial potential in early periods of treatment (4 and 24 h), but that which intensifies over longer periods of treatment and later become sufficient to release this pro-apoptotic factor. The cytochrome-c released into cytosol and forms a complex with APAF-1 and pro-caspase-9, called the apoptosome, which promotes the cleavage of pro-caspase-9 and the release of active caspase-9 [44]. Once activated, caspase-9 activates caspase-3, which leads to apoptosis [45]. The activation of caspases could be involved in mechanism of action of Amblyomin-X, since its cytotoxicity was blocked by caspases inhibitors and Amblyomin-X treatment caused caspase-3/7 activation and PARP cleavage. However, in SK-MEL-28 cells, cleavage of PARP was detected prior to the release of cytochrome-c, suggesting the activation of caspase-3 pathway through other components, such as ER stress (caspase-4) and death (caspase-8) [32].

Even with all this evidence, it is not possible to establish a clear relationship between ER stress, elevations of $[Ca^{2+}]_i$, mitochondrial dysfunction, and caspase activation induced by Amblyomin-X. Notwithstanding, there is no way of ruling out the possibility of activation of these pathways separately by Amblyomin-X, and that their individual cellular response converge in apoptosis, or proceed until reaching the point of synergy among the pathways. However, more investigations are necessary to define the sequence of these events. In conclusion, these investigations might help in further understanding of the antitumor properties of Amblyomin-X, which has potential to become a promising candidate for the treatment of cancer.

Conclusion

Many investments and efforts are made to improve cancer therapy; for example, in recent years, dozens of proteasome inhibitors have been synthesized and studied. Herein, we have demonstrated that Amblyomin-X, a proteasome inhibitor disturbs cell homeostasis and overlaps the tumor resistance mechanisms, culminating in cell death. Although cells upon Amblyomin-X treatment present differences in time and intensity of pro-apoptotic effects, the mechanism of action observed is similar in the tumor cells studied. Interestingly, all investigations on Amblyomin-X have shown its toxicity to tumor cells, but not to normal human fibroblasts cells, reinforcing its selectivity to tumor cells. Thus, Amblyomin-X could be a promising candidate for the treatment and study of cancer.

Experimental section

Amblyomin-X production

The homogeneous recombinant protein was prepared as reported elsewhere [25].

Cell lines and culture conditions

Human's melanomas (SK-MEL-28 and SK-MEL-5) and pancreatic adenocarcinomas (MIA-PaCa-2, Panc1, BxPC3, AsPC1) cells were obtained and cultured according to instructions of American type culture collection (ATCC, Manassas, VA). Human normal fibroblasts were isolated from biopsy dermal tissue of adult subjects. Cells were maintained in Dulbecco's Modified Eagle Medium (DMEM) supplemented with 15 % fetal bovine serum and 1 % of antibiotic solution (0.1 mg/mL of streptomycin and 100U/mL of penicillin). All cell lines were routinely grown in a humidified 5 % CO_2 incubator at 37 °C.

Cell viability assay

Cell viability was measured by MTT tests as described elsewhere [24]. In order to investigate the caspase inhibitors or chelating intracellular calcium, SK-MEL-28 and Mia-PaCa-2 cells were seeded in 96-well plates (10^4 cells/well) and pre-incubated with specific caspase-3 inhibitor DEVD-CHO (10 μM), pan caspase inhibitor ZVAD-FMK (50 μM), or with BAPTA-AM (10 μM) for 30 min. Finally, cell viability was measured by MTT assay.

Quantitative real-time PCR analysis

Tumor cells (SK-MEL-28 and Mia-PaCa-2) and human fibroblast were harvested at various time points after treatment with Amblyomin-X. Subsequently, the total RNA was extracted from these cells lines using the RNeasy kit (Qiagen, Netherlands) and DNase treatment was carried

out. Then, cDNA strands were constructed using a SuperScript® III First-Strand Synthesis kit (Invitrogen™, Life Technologies Inc., USA), according to manufacturer's instructions. Finally, the samples were applied in a SYBR® green (Applied Biosystems, USA)-based reaction with specific and validated primers to evaluate mRNA levels of genes coding for ER stress proteins. The GAPDH (Glyceraldehyde-3-phosphate dehydrogenase) gene expression level was used as normalize control. The experiments were conducted by Step One Plus® PCR real-time system (Applied Biosystems, USA) with the following cycle conditions: 10 min at 95 °C, followed by 40 cycles of denaturation of 15 s at 95 °C, 30 s at 60 °C, and finally 30 s at 72 °C. The relative mRNA levels of gene expression were calculated using the Pfaffl method [46].

Indirect immunofluorescence

ER stress-induced transport ATF-6α was verify according previous reports [47]. Tumor cells were grown on coverslips in 15×15 mm 6-well plate and treated with Amblyomin-X (1 μM) for 4 and 24 h; or MG-132 (2.5 μM) for 24 h, a known proteasome inhibitor; or thapsigargin (1 μM) for 24 h, a selective inhibitor of endoplasmic reticulum Ca2+-ATPase, which was reported to induce ER stress. Cells were washed twice with 1X PBS and fixed with 4 % paraformaldehyde for 15 min at room temperature. The washing step was repeated and, then cells were incubated with a cell permeabilization solution (0.1 % saponin in PBS 1X) for 15 min at room temperature. Samples were washed and were incubated with blocking solution 1 % BSA for 30 min at room temperature. Following, the primary antibody was incubated overnight at 4 °C in (i) anti- human- ERGIC 53 mouse (Origen, Netherlands) 1:100; (ii) anti-human ATF-6α rabbit (Santa Cruz Biotechnology, Inc., USA) 1:50. A washing procedure was carried out and samples were incubated with secondary antibodies Alexa Fluor® 555 goat anti-rabbit (Invitrogen™ Life Technologies Inc., USA), and Alexa Fluor ® 488 rabbit anti-mouse (Invitrogen™ Life Technologies Inc., USA), both at 1:200 dilution for 1 h at room temperature in the dark. Cells were washed and one drop of solution anti-fade mounting VECTASHIELD® (Vector Labs, USA) was applied on the slide with cover slip containing cells facing down and, then, sealed. The analysis was performed in LSMS Zeiss 510 confocal microscope (Zeiss, Germany).

Western blot analysis

Total cellular proteins were extracted from tumor cells treated with Amblyomin-X or PBS 1X (Ctrl) using strong RIPA lysis buffer (150 mM NaCl, 1.0 % IGEPAL® CA-630, 0.5 % sodium deoxycholate, 0.1 % SDS, and 50 mM Tris, pH 8.0.) and were quantified by BCA (bicinchoninic acid assay) using the Pierce® Microplate BCA Protein Assay kit (Thermo Scientific, USA). Then, protein samples (30 μg) were subjected to standard SDS-PAGE and were transferred onto a polyvinylidene difluoride membrane (GE Healthcare, USA). For detection of protein of interest, primary polyclonal antibodies were applied on membrane. Primary antibodies used were anti-GRP78 (Santa Cruz Biotechnology, Inc., CA, USA), anti-GADD153 (Santa Cruz Biotechnology, Inc., USA), anti-PARP (Cell Signaling, MA, USA), and anti-GAPDH (Sigma-Aldrich, MO, USA). Bound antibodies were detected by chemoluminescence method *using* a homemade solution (1.5 M Tris pH 8.9; 20 mM *p*-coumaric acid, 125 mM luminol, and 30 % peroxide hydrogen). The images were acquired at each 10 s exposure in the LAS 4000 equipment (GE Healthcare, USA), employing the ImageQuant® software.

Preparation of protein extract for cytochrome-c measurement

SK-MEL-28 and Mia-PaCa-2 cells were treated with Amblyomin-X. Cells were harvested and were washed twice in PBS. For cytoplasmic cytochrome-c measurement, a modified extraction procedure was used compared to the one we employed for the analysis of GRP78, GADD153, and PARP. Briefly, to obtain a cytoplasmic proteins fraction, cells were re-suspended in relatively weak lysis buffer (HEPES–KOH 10 mM; pH 7.4, EDTA 0.1 mM; bis-etilenoglicol (β-aminoethyl ether); EGTA 1 mM; sucrose 250 mM; orthovanadate (Na3VO4) 1 mM, PMSF 1.0 mM, and dithiothreitol (DTT) 10 mM) and were incubated on ice for 15 min. Samples were then centrifuged at 10,000 g for 15 min at 4 °C to sediment unbroken cells, nuclei, and the heavy membrane fractions containing mitochondria or other cellular compartments. Supernatants containing mostly cytoplasmic proteins were collected and were subjected to immunoblot analysis using anti-cytochrome-c (Santa Cruz Biotechnology, Inc., USA).

Measurements of changes in free intracellular calcium concentration ($[Ca^{2+}]_i$) by microfluorimetry

Changes in cytosolic calcium concentration ($[Ca^{2+}]_i$) were monitored by microfluorimetry, described elsewhere [48]. For this purpose, SK-MEL-28 and human fibroblast cells were transferred into 96 black-well plates (Costar, UK) at a density of 5×10^4 cells per well in serum-free medium. Cells were then kept with FlexStation Calcium Kit containing 2.5 mM probenecid for 60 min at 37 °C. Before and after addition of Amblyomin-X or TAPS, fluorescence

of samples was excited at 485 nm, and fluorescence emission was measured at 525 nm.

Measurement of intracellular Ca²⁺ levels by flow cytometry

Tumor cells (SK-MEL-28 and Mia-PaCa-2) were grown with 0.5 μM Amblyomin-X or PBS for 4 and 24 h. Cells were washed with PBS, and incubated with 10 μM of calcium green-1-AM (Molecular Probes, OR). Calcium green-1-AM is labeled with calcium indicator molecule that changes fluorescence upon binding Ca^{2+} in the presence of 0.2 % of non-ionic surfactant pluronic acid F-127 (Sigma-Aldrich, MO, USA). Stained cells were examined on flow cytometer FACSCalibur (Becton, Dickinson and Company, CA, USA). For data analyses, FlowJo (FlowJo, LLC, OR, USA) software was employed.

Mitochondrial potential measured

The rhodamine 123 (^{123}Rh) is a lipophilic cationic fluorochrome that is readily incorporated into mitochondria in manner-dependent mitochondrial membrane potential [49, 50]. It is a cationic fluorochrome, which is attracted by a high negative electrical potential present in the mitochondrial membrane. Changes in mitochondrial membrane integrity cause diffusion of ^{123}Rh from mitochondria to cytosol and it can be detected by a decrease in fluorescence [49, 50]. Briefly, after 4 or 24 h of Amblyomin-X treatment (0.5 μM), the tumor cells (SK-MEL-28 and Mia-PaCa-2) and human fibroblast cells (10^5 cells/plate) were suspended in 300 μL FACs buffer and incubated with ^{123}Rh probe (200 ng/mL) in a humidified 5 % CO2 incubator for 30 min at 37 °C. Finally, cells were washed in cold PBS, and mitochondrial potential was measured using a flow cytometer FACSCalibur (Becton e Dickson, CA, USA). For data analyses, FlowJo (FlowJo, LLC, OR, USA) software was employed.

Caspase activation

To verify caspase activity, CellEvent™ Caspase-3/7 Green Detection Reagent (Molecular Probes Inc. USA) was used according to manufacturer's instructions. Briefly, tumor cells were treated with Amblyomin-X (1 μM) for 4 and 24 h; or with MG-132 (2.5 μM) for 24 h; or with TAPS (1 μM) for 24 h. Then, tumor cells were stained with CellEvent™ Caspase-3/7 Green Detection Reagent for 30 min at 37 °C. The fluorogenic response resulting from DEVD peptide cleavage was measured by flow cytometer FACSCalibur (Becton e Dickson, CA, USA). For data analyses, FlowJo (FlowJo, LLC, OR, USA) software was employed.

Statistical analysis

Comparisons were carried out using Two-way ANOVA analysis followed by Tukey's Post Hoc test or t-Test, employing the GraphPad Prism 5.0 software (GraphPad Software Inc., San Diego, CA). The criteria for statistical significance were set up as $*p \leq 0.05$, $**p \leq 0.01$, and $***p \leq 0.001$.

Compliance with ethical standards

References

1. Ding F, Xiao H, Wang M, Xie X, Hu F (2014) The role of the ubiquitin-proteasome pathway in cancer development and treatment. Front Biosci (Landmark Ed) 19:886–895

2. Reinstein E, Ciechanover A (2006) Narrative review: protein degradation and human diseases: the ubiquitin connection. Ann Intern Med 145:676–684

3. de Bettignies G, Coux O (2010) Proteasome inhibitors: dozens of molecules and still counting. Biochimie 92:1530–1545. doi:10.1016/j.biochi.2010.06.023

4. Nawrocki ST, Sweeney-Gotsch B, Takamori R, McConkey DJ (2004) The proteasome inhibitor bortezomib enhances the activity of docetaxel in orthotopic human pancreatic tumor xenografts. Mol Cancer Ther 3:59–70

5. Fribley A, Zeng Q, Wang CY (2004) Proteasome inhibitor PS-341 induces apoptosis through induction of endoplasmic reticulum stress-reactive oxygen species in head and neck squamous cell carcinoma cells. Mol Cell Biol 24:9695–9704. doi:10.1128/MCB.24.22.9695-9704.2004

6. Mimura N, Hideshima T, Shimomura T, Suzuki R, Ohguchi H, Rizq O, Kikuchi S, Yoshida Y, Cottini F, Jakubikova J, Cirstea D, Gorgun G, Minami J, Tai YT, Richardson PG, Utsugi T, Iwama A, Anderson KC (2014) Selective and potent Akt inhibition triggers anti-myeloma activities and enhances fatal endoplasmic

reticulum stress induced by proteasome inhibition. Cancer Res 74:4458–4469. doi:10.1158/0008-5472.CAN-13-3652

7. Vaeteewoottacharn K, Kariya R, Matsuda K, Taura M, Wongkham C, Wongkham S, Okada S (2013) Perturbation of proteasome function by bortezomib leading to ER stress-induced apoptotic cell death in cholangiocarcinoma. J Cancer Res Clin Oncol 139:1551–1562. doi:10.1007/s00432-013-1473-6

8. Boelens J, Lust S, Offner F, Bracke ME, Vanhoecke BW (2007) Review. The endoplasmic reticulum: a target for new anticancer drugs. In Vivo 21:215–226

9. Lai E, Teodoro T, Volchuk A (2007) Endoplasmic reticulum stress: signaling the unfolded protein response. Physiology (Bethesda) 22:193–201. doi:10.1152/physiol.00050.2006

10. Demasi M, Laurindo FR (2012) Physiological and pathological role of the ubiquitin-proteasome system in the vascular smooth muscle cell. Cardiovasc Res 95:183–193. doi:10.1093/cvr/cvs128

11. Martinon F (2012) Targeting endoplasmic reticulum signaling pathways in cancer. Acta Oncol 51:822–830. doi:10.3109/0284186X.2012.689113

12. Ron D, Walter P (2007) Signal integration in the endoplasmic reticulum unfolded protein response. Nat Rev Mol Cell Biol 8:519–529. doi:10.1038/nrm2199

13. Bertolotti A, Zhang Y, Hendershot LM, Harding HP, Ron D (2000) Dynamic interaction of BiP and ER stress transducers in the unfolded-protein response. Nat Cell Biol 2:326–332. doi:10.1038/35014014

14. Ellgaard L, Helenius A (2003) Quality control in the endoplasmic reticulum. Nat Rev Mol Cell Biol 4:181–191. doi:10.1038/nrm1052

15. Rutkowski DT, Kaufman RJ (2004) A trip to the ER: coping with stress. Trends Cell Biol 14:20–28

16. Rasheva VI, Domingos PM (2009) Cellular responses to endoplasmic reticulum stress and apoptosis. Apoptosis 14:996–1007. doi:10.1007/s10495-009-0341-y

17. Orrenius S, Zhivotovsky B, Nicotera P (2003) Regulation of cell death: the calcium-apoptosis link. Nat Rev Mol Cell Biol 4:552–565. doi:10.1038/nrm1150

18. Hetz C, Bernasconi P, Fisher J, Lee AH, Bassik MC, Antonsson B, Brandt GS, Iwakoshi NN, Schinzel A, Glimcher LH, Korsmeyer SJ (2006) Proapoptotic BAX and BAK modulate the unfolded protein response by a direct interaction with IRE1alpha. Science 312:572–576. doi:10.1126/science.1123480

19. Oyadomari S, Mori M (2004) Roles of CHOP/GADD153 in endoplasmic reticulum stress. Cell Death Differ 11:381–389. doi:10.1038/sj.cdd.4401373

20. Faitova J, Krekac D, Hrstka R, Vojtesek B (2006) Endoplasmic reticulum stress and apoptosis. Cell Mol Biol Lett 11:488–505. doi:10.2478/s11658-006-0040-4

21. Gerasimenko J, Ferdek P, Fischer L, Gukovskaya AS, Pandol SJ (2010) Inhibitors of Bcl-2 protein family deplete ER Ca2+ stores in pancreatic acinar cells. Pflugers Arch 460:891–900. doi:10.1007/s00424-010-0859-4

22. Green DR, Kroemer G (2004) The pathophysiology of mitochondrial cell death. Science 305:626–629. doi:10.1126/science.1099320

23. Zong WX, Li C, Hatzivassiliou G, Lindsten T, Yu QC, Yuan J, Thompson CB (2003) Bax and Bak can localize to the endoplasmic reticulum to initiate apoptosis. J Cell Biol 162:59–69. doi:10.1083/jcb.200302084

24. Batista IF, Chudzinski-Tavassi AM, Faria F, Simons SM, Barros-Batestti DM, Labruna MB, Leao LI, Ho PL, Junqueira-de-Azevedo IL (2008) Expressed sequence tags (ESTs) from the salivary glands of the tick Amblyomma cajennense (Acari: Ixodidae). Toxicon 51:823–834. doi:10.1016/j.toxicon.2007.12.011

25. Batista IF, Ramos OH, Ventura JS, Junqueira-de-Azevedo IL, Ho PL, Chudzinski-Tavassi AM (2010) A new Factor Xa inhibitor from Amblyomma cajennense with a unique domain composition. Arch Biochem Biophys 493:151–156. doi:10.1016/j.abb.2009.10.009

26. Chudzinski-Tavassi AM, De-Sa-Junior PL, Simons SM, Maria DA, de Souza Ventura J, Batista IF, Faria F, Duraes E, Reis EM, Demasi M (2010) A new tick Kunitz type inhibitor, Amblyomin-X, induces tumor cell death by modulating genes related to the cell cycle and targeting the ubiquitin-proteasome system. Toxicon 56:1145–1154. doi:10.1016/j.toxicon.2010.04.019

27. Maria DA, de Souza JG, Morais KL, Berra CM, Zampolli Hde C, Demasi M, Simons SM, de Freitas Saito R, Chammas R, Chudzinski-Tavassi AM (2013) A novel proteasome inhibitor acting in mitochondrial dysfunction, ER stress and ROS production. Investig New Drugs 31:493–505. doi:10.1007/s10637-012-9871-1

28. Nawrocki ST, Carew JS, Dunner K Jr, Boise LH, Chiao PJ, Huang P, Abbruzzese JL, McConkey DJ (2005) Bortezomib inhibits PKR-like endoplasmic reticulum (ER) kinase and induces apoptosis via ER stress in human pancreatic cancer cells. Cancer Res 65:11510–11519. doi:10.1158/0008-5472.CAN-05-2394

29. Pacheco MT, Berra CM, Morais KL, Sciani JM, Branco VG, Bosch RV, Chudzinski-Tavassi AM (2014) Dynein function and protein clearance changes in tumor cells induced by a Kunitz-type molecule, Amblyomin-X. PLoS One 9:e111907. doi:10.1371/journal.pone.0111907

30. Bannykh SI, Balch WE (1997) Membrane dynamics at the endoplasmic reticulum-Golgi interface. J Cell Biol 138:1–4

31. Hauri HP, Kappeler F, Andersson H, Appenzeller C (2000) ERGIC-53 and traffic in the secretory pathway. J Cell Sci 113(Pt 4):587–596

32. Fiandalo MV, Kyprianou N (2012) Caspase control: protagonists of cancer cell apoptosis. Exp Oncol 34:165–175

33. D'Amours D, Desnoyers S, D'Silva I, Poirier GG (1999) Poly(-ADP-ribosyl)ation reactions in the regulation of nuclear functions. Biochem J 342(Pt 2):249–268

34. Lazebnik YA, Kaufmann SH, Desnoyers S, Poirier GG, Earnshaw WC (1994) Cleavage of poly(ADP-ribose) polymerase by a proteinase with properties like ICE. Nature 371:346–347. doi:10.1038/371346a0

35. Decker P, Muller S (2002) Modulating poly (ADP-ribose) polymerase activity: potential for the prevention and therapy of pathogenic situations involving DNA damage and oxidative stress. Curr Pharm Biotechnol 3:275–283

36. Deer EL, Gonzalez-Hernandez J, Coursen JD, Shea JE, Ngatia J, Scaife CL, Firpo MA, Mulvihill SJ (2010) Phenotype and genotype of pancreatic cancer cell lines. Pancreas 39:425–435. doi:10.1097/MPA.0b013e3181c15963

37. Yunis AA, Arimura GK, Russin DJ (1977) Human pancreatic carcinoma (MIA PaCa-2) in continuous culture: sensitivity to asparaginase. Int J Cancer 19:128–135

38. Chen WH, Horoszewicz JS, Leong SS, Shimano T, Penetrante R, Sanders WH, Berjian R, Douglass HO, Martin EW, Chu TM (1982) Human pancreatic adenocarcinoma: in vitro and in vivo morphology of a new tumor line established from ascites. In Vitro 18:24–34

39. Ma XH, Piao SF, Dey S, McAfee Q, Karakousis G, Villanueva J, Hart LS, Levi S, Hu J, Zhang G, Lazova R, Klump V, Pawelek JM, Xu X, Xu W, Schuchter LM, Davies MA, Herlyn M, Winkler J, Koumenis C, Amaravadi RK (2014) Targeting ER stress-induced autophagy overcomes BRAF inhibitor resistance in melanoma. J Clin Investig 124:1406–1417. doi:10.1172/JCI70454

40. Davies H, Bignell GR, Cox C, Stephens P, Edkins S, Clegg S, Teague J, Woffendin H, Garnett MJ, Bottomley W, Davis N, Dicks E, Ewing R, Floyd Y, Gray K, Hall S, Hawes R, Hughes J, Kosmidou V, Menzies A, Mould C, Parker A, Stevens C, Watt S, Hooper S, Wilson R, Jayatilake H, Gusterson BA, Cooper C,

Shipley J, Hargrave D, Pritchard-Jones K, Maitland N, Chenevix-Trench G, Riggins GJ, Bigner DD, Palmieri G, Cossu A, Flanagan A, Nicholson A, Ho JW, Leung SY, Yuen ST, Weber BL, Seigler HF, Darrow TL, Paterson H, Marais R, Marshall CJ, Wooster R, Stratton MR, Futreal PA (2002) Mutations of the BRAF gene in human cancer. Nature 417:949–954. doi:10.1038/nature00766

41. Fernandez Y, Verhaegen M, Miller TP, Rush JL, Steiner P, Opipari AW Jr, Lowe SW, Soengas MS (2005) Differential regulation of noxa in normal melanocytes and melanoma cells by proteasome inhibition: therapeutic implications. Cancer Res 65:6294–6304. doi:10.1158/0008-5472.CAN-05-0686

42. Lu S, Wang J (2013) The resistance mechanisms of proteasome inhibitor bortezomib. Biomark Res 1:13. doi:10.1186/2050-7771-1-13

43. Ruschak AM, Slassi M, Kay LE, Schimmer AD (2011) Novel proteasome inhibitors to overcome bortezomib resistance. J Natl Cancer Inst 103:1007–1017. doi:10.1093/jnci/djr160

44. Wu Z, Lu Y, Wang B, Liu C, Wang ZR (2003) Effects of bile acids on proliferation and ultrastructural alteration of pancreatic cancer cell lines. World J Gastroenterol 9:2759–2763

45. Petros AM, Olejniczak ET, Fesik SW (2004) Structural biology of the Bcl-2 family of proteins. Biochim Biophys Acta 1644:83–94. doi:10.1016/j.bbamcr.2003.08.012

46. Pfaffl MW (2001) A new mathematical model for relative quantification in real-time RT-PCR. Nucleic Acids Res 29:e45

47. Nadanaka S, Yoshida H, Kano F, Murata M, Mori K (2004) Activation of mammalian unfolded protein response is compatible with the quality control system operating in the endoplasmic reticulum. Mol Biol Cell 15:2537–2548. doi:10.1091/mbc.E03-09-0693

48. Morais KL, Ianzer D, Miranda JR, Melo RL, Guerreiro JR, Santos RA, Ulrich H, Lameu C (2013) Proline rich-oligopeptides: diverse mechanisms for antihypertensive action. Peptides 48:124–133. doi:10.1016/j.peptides.2013.07.016

49. Benel L, Ronot X, Kornprobst M, Adolphe M, Mounolou JC (1986) Mitochondrial uptake of rhodamine 123 by rabbit articular chondrocytes. Cytometry 7:281–285. doi:10.1002/cyto.990070309

50. Johnson LV, Walsh ML, Chen LB (1980) Localization of mitochondria in living cells with rhodamine 123. Proc Natl Acad Sci USA 77:990–994